

Dynamic hysteresis scaling of first-order phase transition ferroelectrics near the phase transition point in the $(\eta^2)^3$ model

This article has been downloaded from IOPscience. Please scroll down to see the full text article.

2003 J. Phys.: Condens. Matter 15 8631

(<http://iopscience.iop.org/0953-8984/15/49/032>)

View [the table of contents for this issue](#), or go to the [journal homepage](#) for more

Download details:

IP Address: 171.66.16.125

The article was downloaded on 19/05/2010 at 17:52

Please note that [terms and conditions apply](#).

Dynamic hysteresis scaling of first-order phase transition ferroelectrics near the phase transition point in the $(\eta^2)^3$ model

H Yu^{1,2}, Y Wang^{1,2}, J-M Liu^{1,2,4}, H L W Chan^{1,3} and C L Choy^{1,3}

¹ Laboratory of Solid State Microstructures, Nanjing University, Nanjing 210093, People's Republic of China

² International Centre for Materials Physics, Chinese Academy of Sciences, Shenyang, People's Republic of China

³ Department of Applied Physics, Hong Kong Polytechnic University, Hong Kong, People's Republic of China

E-mail: liujm@nju.edu.cn

Received 17 August 2003, in final form 28 October 2003

Published 25 November 2003

Online at stacks.iop.org/JPhysCM/15/8631

Abstract

The dynamic hysteresis of the first-order phase transition around the transition point T_c in ferroelectrics is studied by investigating the dynamic response of the Landau–Devonshire $(\eta^2)^3$ model to a time-varying external field of frequency f and amplitude E_0 . It is revealed that the single-loop hysteresis as obtained above the upper critical point T^+ and below the absolute instability point T_0 shows dynamic behaviours very different from the double-loop hysteresis obtained between T_c and T^+ . An extensive calculation reveals a power-law scaling for hysteresis area as a function of E_0 , while no reliable power-law scaling for the area as a function of f is available in the low- f regime. The scaling for the double-loop hysteresis seems not to fall into the same class as single-loop hysteresis. Furthermore, the power-law exponents, if any, are somewhat temperature-dependent, but this dependence is very weak in the regime of low E_0 and high f .

1. Introduction

Hysteresis represents the intrinsic feature of dynamic non-equilibrium phase transitions in a wide class of ferroic materials. In this paper, we are interested in the problem of dynamic hysteresis that has been receiving attention not only for physical interests in the last decades. Dynamic hysteresis originates from the dependence of the hysteresis on the frequency f and amplitude E_0 of the external field. Practically, high-speed memory and sensing applications

⁴ Author to whom any correspondence should be addressed.

where ferroic materials are employed require a comprehensive knowledge of the dynamic hysteresis in these materials [1]. However, the problem of dynamic hysteresis was not emphasized until the last ten years. For a detailed review of the latest progress on this topic, refer to the review article of Chakrabarti and Acharyya [2]. On the other hand, the scaling behaviour of the hysteresis dispersion characterizes the frequency or amplitude dispersion of hysteresis area A , i.e. $A(f)$ at a fixed E_0 , or $A(E_0)$ at a given f . The earliest empirical scaling behaviour is known as the Steinmetz law [3] for ferrites. Rao *et al* [4, 5] presented a systematic study on the hysteresis dispersion in $O(N \rightarrow \infty)$ -symmetric $(\eta^2)^2$ and $(\eta^2)^3$ models at a temperature T far below the phase transition point T_c . A power-law scaling for the dispersion against both f and E_0 in either the low- f or high- f regime was argued. Subsequently, different dispersions were identified for various models, where the Ising model was chosen as the base for MFA (mean-field approach) studies [6–8] and MC (Monte Carlo) simulation [4, 9–11]. Dhar and Thomas [12, 13] studied the hysteresis scaling in small systems under a low field, and predicted that $A(f)$ over the low- f regime is logarithmic. The finite-size scaling of the dynamic hysteresis was presented by Sides *et al* [14, 15], while Zhong and Zhang employed renormalization-group theory to study the same problem [16]. A number of recent works claimed that some scaling function of hysteresis such as $A(f, E_0) = E_0^\alpha f^\beta$ exists, although some critical works also argued the invalidity of such power-law scaling. Acharyya and his co-workers [2, 17] took the thermal fluctuations into account and obtained a general dispersion for $T > T_c$:

$$A(f, H_0, T) \propto H_0^a T^{-m} g\left(\frac{f}{H_0^c T^n}\right) \quad (1)$$

$$g\left(\tilde{f} = \frac{f}{H_0^c T^n}\right) \propto \tilde{f}^b \exp(-\tilde{f}^2/\sigma)$$

where m, n, a, b and c are the scaling exponents. For $f \rightarrow 0$, equation (1) reduces to a power law. The experimental data on several thin-film magnets [18–20] can be reasonably fitted by equation (1) with variable exponents for various systems.

The main motivation of our work is to find the hysteresis behaviours in ferroelectrics of the first-order phase transition around T_c , which benefits our understanding of the dynamics of ferroelectric systems near the phase transition point but few reports have been found on this subject. An earlier systematic work [21] on double hysteresis loops in ferroelectrics LiCsSO_4 in general presented static aspects of this phenomenon.

To date, most works have focused on the dynamic hysteresis in spin systems at $T \ll T_c$, and the static property related to hysteresis for the second-order phase transition. In the present paper, the $(\eta^2)^3$ model was used to investigate dynamic hysteresis in ferroelectrics and general first-order phase transition systems. A detailed study for both $(\eta^2)^2$ and $(\eta^2)^3$ models in a three-dimensional continuous N -component system ($N \rightarrow \infty$) at $T \ll T_c$ was presented by Rao *et al* [4, 5]. They argued that the scaling behaviour for both models is in the same universality class, which may be true in case of $T \ll T_c$, because the dynamics for both can be described by the domain reversal mechanism. Our main argument is that around T_c the $(\eta^2)^3$ model may show essentially different behaviours from those at $T \ll T_c$ because of the complexity of free energy as a function of T and order parameter near T_c . We pay more attention to the phenomena near or above T_c by considering the coexistence of two phases (ferro- and paraelectric phases) which introduces the diversities of hysteresis loops induced by external field and temperature.

The calculation of this paper reveals a scaling behaviour of single and double hysteresis area as a function of E_0 and f . No reliable power law was found for saturated double loops in ordinary frequency and field. However, for high frequency or low field, the loop types

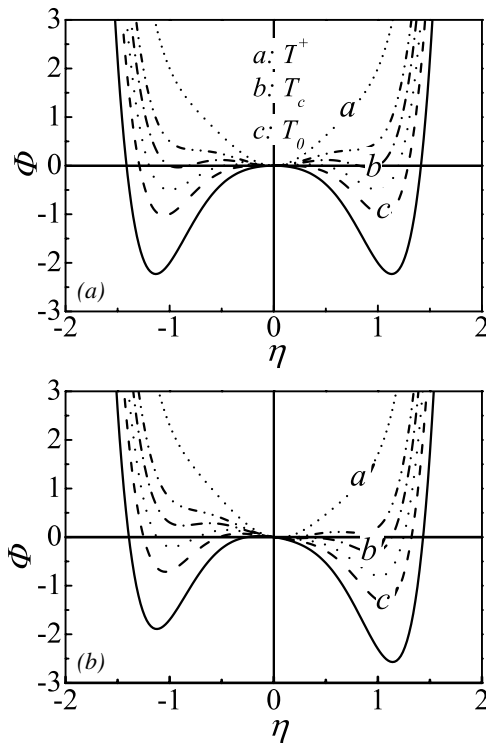


Figure 1. Landau–Devonshire free energy potential. (a) Without external field: a, $T-T^+$; b, $T-T_c$; c, $T-T_0$. (b) With external field.

are similarly non-saturated and the exponents are invariable and independent of temperature. From the point of view of applications in high-speed ferroelectric memories, the invariable scaling exponents for high frequency (with exponent $\beta = -1.00$) and low field ($\alpha = 2.00$) may be significant.

2. $O(N = \infty)$ -symmetric $(\eta^2)^3$ model and numerical method

We begin this model from Landau–Devonshire theory [22] which applies to the case of weak first-order phase transitions often identified for ferroelectrics. The free energy function takes the following form:

$$\Phi(T, \eta) = \Phi_0 + a(T - T_0)\eta^2 + B\eta^4 + D\eta^6 + h\eta \quad (2)$$

where $a > 0$, $B < 0$ and $D > 0$, η is the order parameter, referring to polarization for ferroelectrics, T_0 is the absolutely unstable limit of the disordered phase and h is the external field. We use $r = T - T_0$ to characterize temperature T . To study the temperature-induced phase transition, we consider the case under zero field. Then, the potential energy as a function of η at various T is plotted in figure 1(a). Without external field, one can obtain the minima by setting $\partial\Phi/\partial\eta = 0$ and $\partial^2\Phi/\partial\eta^2 > 0$:

$$\begin{aligned} \eta_0 &= 0, \\ \eta_{\pm} &= \pm \sqrt{\frac{-B + [B^2 - 3aD \cdot (T - T_0)]^{1/2}}{3D}}. \end{aligned} \quad (3)$$

The real value of η requires

$$T^+ = T_0 + \frac{B^2}{3aD} > T_0. \quad (4)$$

For $T < T^+$, the free energy has three minima respectively at $\eta = \eta_0$ and η_{\pm} . By setting $\Phi = \Phi_0$, one has the first critical temperature T_c :

$$T_c = T_0 + \frac{B^2}{4aD} < T^+ \quad (5)$$

which corresponds to the three equivalent minimum states of free energy at $\eta = \eta_0$ and η_{\pm} , respectively. The thermodynamic stability depends on T , in a way described below.

- (1) For $T < T_0$ ($r < 0$), the disordered phase is absolutely unstable, and $a(T - T_0) < 0$. The system prefers the ordered phase with a double-well potential at nonzero η_{\pm} . At η_0 , the energy has a maximum, thus the formed hysteresis is a single loop.
- (2) For $T_0 < T < T_c$, the system has three free energy minima (wells), but the well bottom at η_{\pm} is lower than that at η_0 . The pattern of hysteresis remains single loop but deformed a little.
- (3) For $T_c < T < T^+$, the free energy at η_0 is lower than that at η_{\pm} . The disordered phase ($\eta_0 = 0$) is preferred but the ordered phase (η_{\pm}) still remain metastable. A double-loop hysteresis is observed.
- (4) For $T > T^+$, the free energy no longer shows any minimum at η_{\pm} and $\eta_0 = 0$ remains the uniquely stable state (disordered phase).

Figure 1(b) is the case considering the influence of an external field that breaks the symmetry of the potential well.

The $(\eta^2)^3$ model is based on $O(N)$ continuum generalization of the Heisenberg model ($N = 3$) in the presence of a field [23]. The model was introduced earlier [4, 5], and here only a brief description is given. The order parameter equation of motion takes the Langevin form:

$$\frac{\partial \eta_{\alpha}}{\partial t} = -\Gamma \frac{\delta F}{\delta \eta_{\alpha}} + \varphi_{\alpha} \quad (6)$$

with the Gaussian white noise satisfying

$$\begin{aligned} \langle \varphi_{\alpha}(x, t) \rangle &= 0, \\ \langle \varphi_{\alpha}(x, t) \varphi_{\beta}(x', t') \rangle &= 2\Gamma \delta_{\alpha\beta} \delta(x - x') \delta(t - t') \end{aligned} \quad (7)$$

where $\alpha, \beta = 1, 2, \dots, N$, represent the orientation in the spin space, \mathbf{x} is the spatial coordinate, Γ is the mobility for the spin–lattice relaxation, F represents the free energy under an external field, which can be written as

$$F = \int d^3x \left[\frac{1}{2} J (\nabla \eta_{\alpha} \cdot \nabla \eta_{\alpha}) + \frac{r}{2} (\eta_{\alpha} \eta_{\alpha}) + \frac{u}{4N} (\eta_{\alpha} \eta_{\alpha})^2 + \frac{v}{6N^2} (\eta_{\alpha} \eta_{\alpha})^3 - \sqrt{N} E_{\alpha} \eta_{\alpha} \right] \quad (8)$$

η is an N -component vector and J is the interaction between two components and u and v are the prefactors of the nonlinear terms, which correspond to factors B and D in equation (2). The phase diagram in the r – u plane can be found in [5], and here $u = -25.59$ and $v = 105.28$ are taken if not noticed elsewhere. The external field is in the $\alpha = 1$ direction, i.e., $E_{\alpha} = E \delta_{\alpha,1}$. In

the $N \rightarrow \infty$ limit, this infinite hierarchy of differential equations is truncated. We substitute equation (8) into (6), and obtain the following coupled integrodifferential equations [5]:

$$\begin{aligned} \frac{dP(t)}{dt} &= \frac{1}{2}[A(t)P(t) + E(t)] \\ A(t) &= -(r + uP^2 + uS + vP^4 + 2vP^2S + vS^2) \\ S(t) &= \frac{1}{2\pi^2} \int_0^1 q^2 C_{\perp}(q, t) dq \\ \frac{d}{dt} C_{\perp}(q, t) &= -[q^2 - A(t)]C_{\perp}(q, t) + 1 \\ E(t) &= E_0 \sin(2\pi f \cdot t) \end{aligned} \quad (9)$$

where P is along the $\alpha = 1$ direction, and $C(q, t)$ is the correlation function which has the transverse component $C_{\perp}(q, t)$ ($\alpha \neq 1$) and longitudinal component $C_{11}(q, t)$ ($\alpha = 1$):

$$\begin{aligned} M(t) &= \langle \Phi_1(q, t) \rangle, \\ C_{\perp}(q, t) &= \langle \Phi_{\alpha}(q, t) \Phi_{\alpha}(-q, t) \rangle, \quad \alpha \neq 1, \\ C_{11}(q, t) &= \langle \Phi_1(q, t) \Phi_1(-q, t) \rangle. \end{aligned} \quad (10)$$

In our simulation, $a = 1$, $B = u = -25.59$, $D = v = 105.28$, $r_c = T_c - T_0 = B^2/(3aD) = 1.55$ and $r^+ = T^+ - T_0 = B^2/(4aD) = 2.07$. Under the static limit, the double loop is generated within $1.55 < r < 2.07$, but the upper limit of r will be higher than $r^+ = 2.07$ if a nonzero E is applied, noting that the values of E_0 and f for our simulation only have relative significance.

When a non-zero E is applied, the symmetry of the free energy is broken. If E is time varying, the dynamics becomes more complex, to be discussed in section 4. The dynamic hysteresis originates from the broken symmetry of the system free energy.

3. Simulation results and hysteresis scaling

3.1. Shape evolution of dynamic hysteresis

The pattern and area of the dynamic P - E loop are functions of T , f and E_0 . Consequently, one understands that the scaling behaviours depend on the three variables. The pattern of hysteresis, single or double, depends on T , whilst the area is dependent on f and E_0 at a fixed T . It is understood that a low f and high E_0 benefit a saturated loop. A lower f means that the system has enough time to respond to the oscillating E , while a high E_0 switches more domains and hence enlarges the enclosed curves.

For $T < T_c$, the static hysteresis should be a single loop. The system at extremely low f has enough time to reach the lowest free energy state. The loop is pinched along the E axis and shows a jump from the $+\eta$ state to the $-\eta$ state or vice versa. With increasing f , the pinched loop becomes more saturated and squarish. Correspondingly, the coercivity increases. Given a fixed E_0 , the loop shape at high f is an inclined ellipse. As $f \rightarrow \infty$, the loop shrinks rapidly along the η -axis and the loop area decays rapidly. As an example, several loops calculated at different values of f are presented in figure 2.

For $T_c < T < T^+$, the system has three free-energy minima, whilst a double-loop hysteresis is generated at relatively low f . When f increases, the double-loop evolves into a dumbbell-like loop. The coercivity E_c and loop area A augment with lifted f . Area A becomes decaying if f is further increased, leaving a maximum that corresponds to a resonant frequency. At extremely high f , the loop becomes an ellipse and finally shrinks into an inclined straight line. Figure 3 shows the double-loop patterns, and it is noted that loop (c) is a dumbbell-like

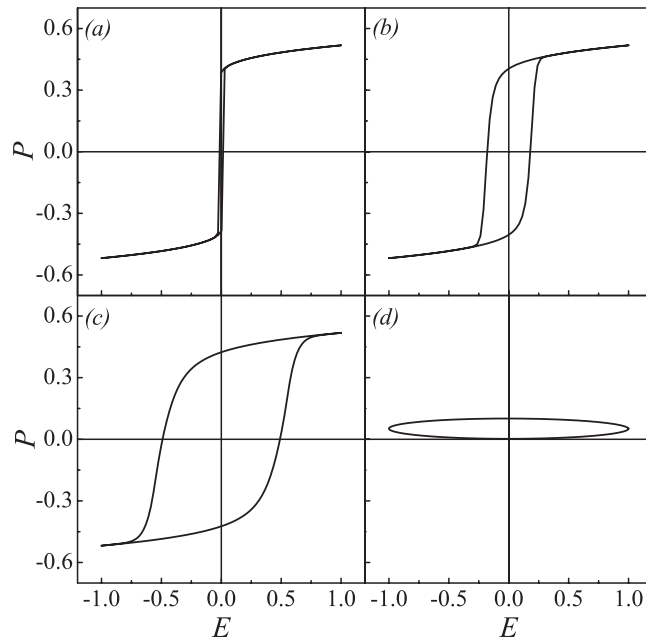


Figure 2. Single-loop hysteresis ($T < T_c$), $r = 1$ and $E_0 = 1$. (a) $f = 0.001$; (b) $f = 0.01$; (c) $f = 0.1$; (d) $f = 10$.

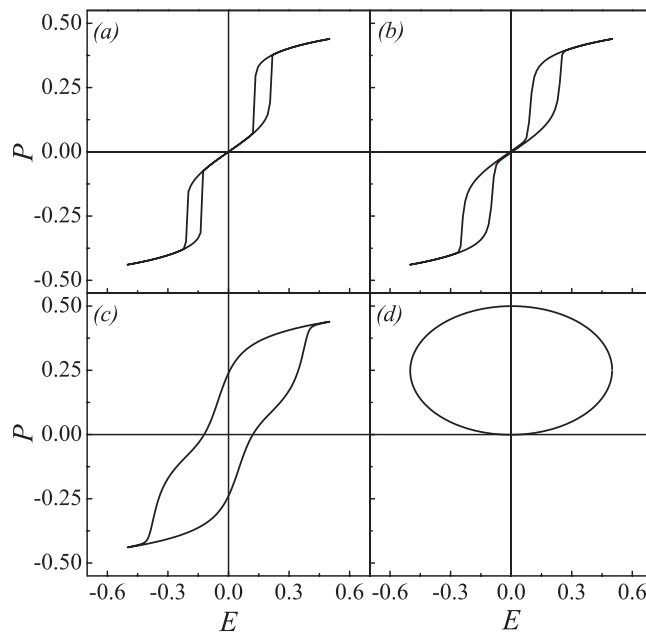


Figure 3. Double-loop hysteresis near T_c ($T_c < T < T^+$), $r = 2$ and $E_0 = 0.5$. (a) $f = 0.001$; (b) $f = 0.01$; (c) $f = 0.1$; (d) $f = 10$.

one. Whether the loop is double is determined by whether η_0 is the minimum when the external field cycles through $E = 0$.

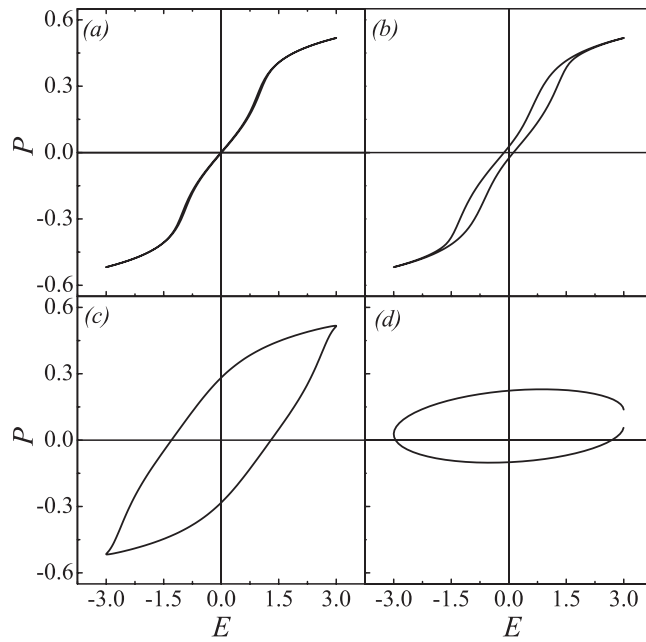


Figure 4. Hysteresis loops at high temperature ($T > T^+$), $r = 5$ and $E_0 = 3$. (a) $f = 0.01$; (b) $f = 0.1$; (c) $f = 1$; (d) $f = 10$.

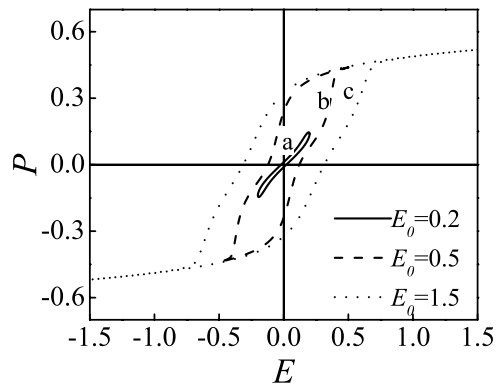


Figure 5. Hysteresis loops under various E_0 as labelled, $r = 2$ and $f = 0.1$.

For $T > T^+$, the high-temperature disordered phase is in the absolutely stable state. The system has one minimum at η_0 , and falls into the paraelectric state, producing a thin and slight loop as shown in figure 4.

In figure 5, we present the hysteresis loops obtained under various E_0 at $r = 2$ and $f = 0.1$, as a demonstration of field-dependent shape evolution. We observe that the loop is minor at relatively small $E_0 = 0.2$, and becomes saturated at $E_0 = 0.5$ and more squarish at $E_0 = 1.5$. The loop at $E_0 = 0.5$ is a dumbbell-like one, which is a transition pattern between single and double ones. This loop will evolve into a single loop with increasing E_0 and a double loop with decreasing f (as shown in figures 3(a)–(c)).

From the results above, we conclude that

- (1) the loop shape at extremely high f remains unsaturated and similar for different regions of temperature, because the system cannot respond to the quickly oscillating field, and
- (2) for very small E_0 , the loop is not saturated, known as a minor loop, which is predicted to obey different scaling laws.

3.2. Scaling behaviours of hysteresis dispersion

Given a system where r , u and v are fixed, the hysteresis area A is a function of f and E_0 , i.e. $A = A(f, E_0)$. As mentioned earlier, a scaling law of the form $A \propto E_0^\alpha f^\beta$ has often been claimed in previous studies. It is essential to check whether this relationship exists or not for the dynamic hysteresis in first-order phase transitions over a broad temperature range covering the critical points defined above. As $T \ll T_0$, the power-law scaling with $\alpha = 2/3$ and $\beta = 1/3$ has been widely confirmed [4, 5]. We pay more attention to the region of two-phase coexistence.

In this simulation, the temperature regimes and the ranges of f and E_0 are wide enough for our investigation to cover all the possibilities of hysteresis. The cases of higher or lower external field and frequency were examined but no new types were found and the shape of the hysteresis loops does not evolve.

Given fixed r and E_0 , area A shows a significant frequency dispersion, which is determined by the competition between the system relaxation time and period of the oscillating field. We present log–log plots in figure 6 of the calculated frequency dispersions. Clearly, no strict universal power law is found at extremely low f ($<10^{-3}$). As f is not very low, we may roughly use a linear fit on the log–log plots over the data on both sides of the mutation point at which $A(f)$ reaches its maximal value, and an exponent β if any is obtained, although this fitting is not very reliable.

Over the low- f range ($f = 10^{-3}$ – 10^{-1}), $\beta > 0$ is temperature dependent. In the range $T_0 < T < T_c$, where the hysteresis is a single loop, the dispersion, as shown in figure 6(a), exhibits an exponent $\beta = 0.47 \pm 0.02$. The linear fit over this range is fairly good, because T is below T_c and more similar to the case at low T . For $T_c < T < T^+$, the hysteresis takes a double-loop pattern, as shown in figure 6(b), no linear relationship and hence no power law if $f < 1$. We argue that the fluctuations at the phase transition point are responsible for the deviation from the simple power law. For $T > T^+$, the loop shrinks into a very thin one. Although the area is small, the dispersion still has an exponent $\beta = 1.00 \pm 0.02$ for $r = 5$ as shown in figure 6(c) and the same value for $r = 7$ in figure 6(d). The loop at high T is inclined to be unsaturated, which can be more easily enlarged by increasing f , hence β is large. Our extensive calculations show that the power-law exponent β , if any, increases as T increases. No universal power law exists for low f over the broad range of T around T_c .

However, over the high- f range where $A(f)$ falls with increasing f , a reliable power law with exponent $\beta = -1.05 \pm 0.04$ independent of T and E_0 is always obtained, confirmed by our extensive calculation covering the wide T -range from $T \ll T_0$ to $T > T^+$. Note that $\beta = -1.0$ at $T \ll T_0$ was confirmed in previous studies [4, 5]; one may argue that a universal frequency power-law scaling applies for the high- f regime. The reason for this universal scaling is related to the fact that the system at any local potential well has a relaxation time longer than $1/f$ so that $A(f)$ is basically dominated by the dynamic response of the system far from the equilibrium state.

The dependence of A on E_0 at a given f was also investigated, as shown in figure 7. A large number of $A(E_0)$ at given f were calculated and four of them ($f = 0.01, 0.1, 10, 100$) are chosen here to show the main features. Because $A(f)$ increases first and then decreases with increasing f , the curves $A(E_0)$ in figure 7 may cross each other. In general, $A(E_0)$ as

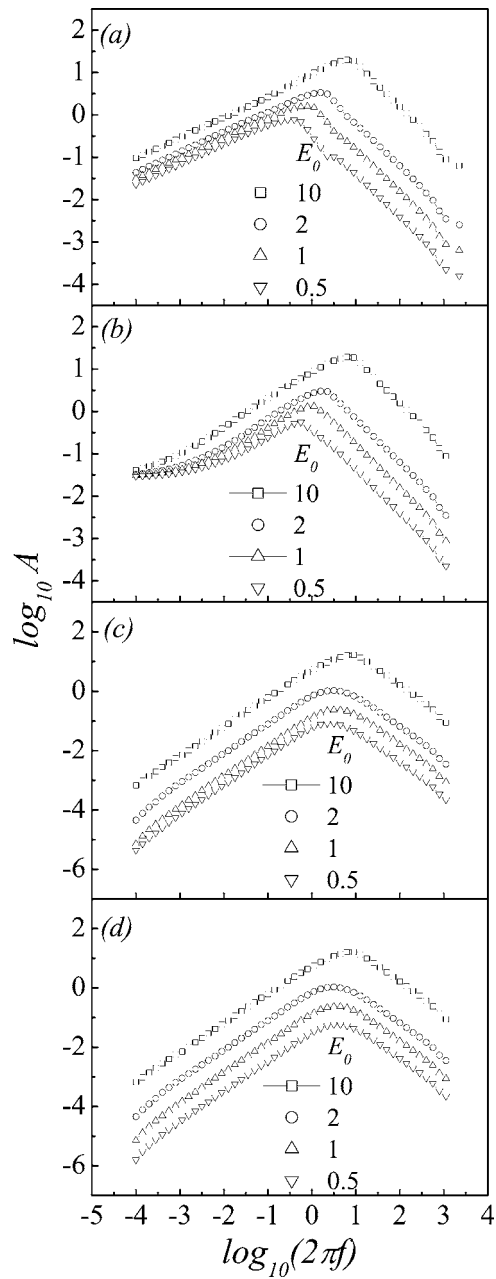


Figure 6. Log-log plots of hysteresis area against frequency f . (a) $r = 1$; (b) $r = 2$; (c) $r = 5$; (d) $r = 7$.

an increasing function of E_0 shows clean linear behaviours in the log-log plots, and there is a mutation point ($E_t, A(E_t)$) for each curve, at which the slope of $A(E_0)$ changes from a small value at $E_0 < E_t$ to a larger one at $E_0 > E_t$. More interesting, one finds that all $A(E_0)$ straight lines at $E_0 < E_t$ and $E_0 > E_t$ in the log-log plots keep parallel to one another, respectively. This means the same slope and hence the same exponent α for all $A(E_0)$ at $E_0 < E_t$ and $E_0 > E_t$, respectively, independent of f .

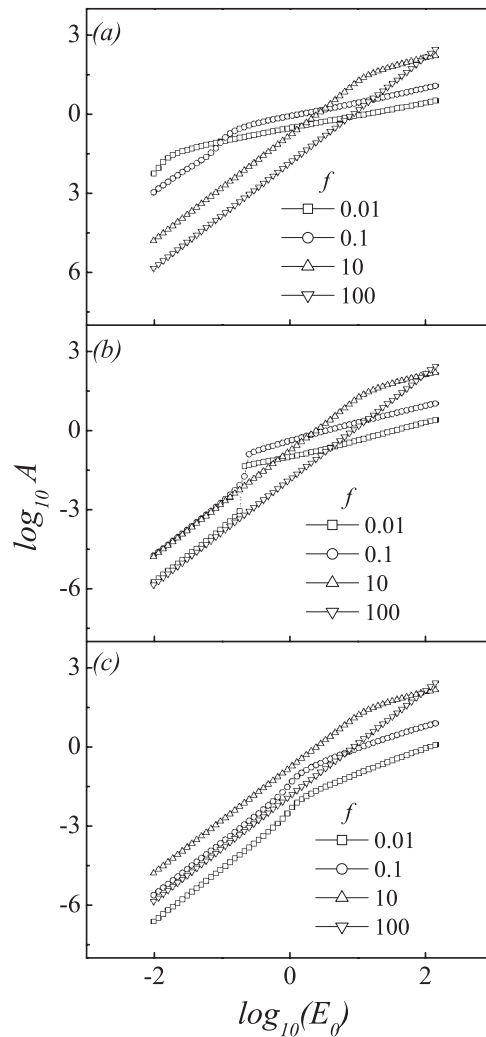














Figure 7. Log–log plots of hysteresis area against amplitude E_0 . (a) $r = 1$; (b) $r = 2$; (c) $r = 5$.

In figure 7, as $E_0 < E_t$, the loops are minor and unsaturated, while the loops at $E_0 > E_t$ are well saturated. At an extremely low amplitude E_0 , the generated loop is unsaturated and irregular. With increasing E_0 , $A(E_0)$ grows rapidly, exhibiting an exponent $\alpha = 2.00 \pm 0.10$ (slope of the straight line at $E < E_t$). It is shown that this exponent does not change for different T and f . As $E_0 > E_t$, the loop is well saturated and a further increasing E_0 does not enhance the remnant polarization much beside enlarging the coercivity, so that exponent α decreases, jumping down from 2.00 to 0.50–0.67. Therefore, E_t can be viewed as the critical amplitude for the complete domain reversal. In contrast, a full domain reversal cannot be achieved if $E_0 < E_t$. E_t is dependent on f , which shifts toward a higher value as f increases. The lower T and lower f benefit saturation of the loop and make E_t smaller. If $f \rightarrow \infty$, the loop is far from saturation but takes an ellipse pattern, hence $E_t \rightarrow \infty$. In such a case, $\alpha \equiv 2.00$.

However, in the case of high E_0 where the loop is well saturated, the case is more complicated. Here, α refers to the slope of the straight line at $E > E_t$. For $0 < r < r_c$,

Table 1. Shape evolutions and scaling behaviours of hysteresis in the first-order $(\eta^2)^3$ system.

T ($r=T-T_0$)	E_0 α	Scaling behaviours $A \propto E_0^\alpha f^\beta$				Potential well ($E>0$)
		Low f		High f		
		Pattern	β	pattern	β	
$*r < 0$	Low f & E_0 0.66 ± 0.03		0.33 ± 0.03		-1.00 ± 0.01	
$0 < r < r_c$	Low E_0 2.00 ± 0.02		0.47 ± 0.02		-1.05 ± 0.01	
	High E_0 0.50 ± 0.02					
$r_c < r < r^+$	Low E_0 2.00 ± 0.01		0.61 ± 0.05 ($f > 10^{-3}$)		-1.07 ± 0.01	
	High E_0 0.64 ± 0.02					
$r > r^+$	Low E_0 2.00 ± 0.02		1.00 ± 0.02		-1.08 ± 0.01	
	High E_0 0.80 ± 0.10					

* $r < 0$ was the work in [4, 5].

E_t is very small for $f = 0.01$ and 0.1 because r is low, as shown in figure 7(a). The hysteresis is single looped and $\alpha = 0.50 \pm 0.04$. For $r_c < r < r^+$, as shown in figure 7(b), the hysteresis is double looped and $\alpha = 0.64 \pm 0.02$. For $r > r^+$, as shown in figure 7(c), $\alpha = 0.80 \pm 0.10$. In short, for a low E_0 and minor loop, α keeps constant in any temperature regime, but different values of α are obtained in different temperature regimes. A lower r benefits the ordered phase, thus favouring a squarish and saturated loop pattern. Therefore, the area increases more slowly and exponent α is lower at lower r .

The evaluated exponents α and β over various ranges of f and E_0 in different temperature regimes are summarized in table 1.

3.3. Remarks on the scaling

We have demonstrated the existence of constant exponents ($\alpha = 2.0$ and $\beta = -1.0$) in the regime of low E_0 and high f , the origin of which is the similar minor loop pattern in these two cases. Apart from this regime, the hysteresis may take different loop patterns, from the single loop, double loop and even dumbbell-like loop over wide ranges of r , E_0 and f . The power-law scaling if any is temperature dependent. Basically, no strict power-law scaling is found for these regimes, although we may still use the power law to scale the dynamics, in the approximate and qualitative senses. These results show clearly that the scaling behaviours of the hysteresis near T_c may not belong to the same generality class as those at much lower temperature. In particular, one understands that the scaling if any for the double-loop hysteresis is very different from the single-loop hysteresis.

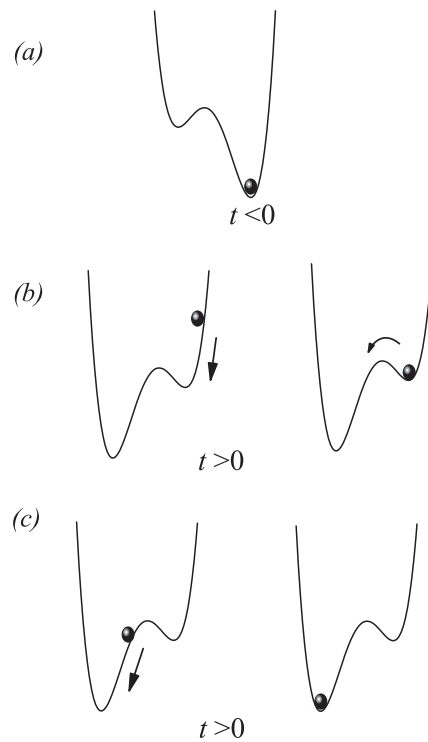


Figure 8. Mechanical analogy and dynamic double-well of free-energy potential (reproduced from [4]). (a) $t < 0$; the particle is in the η_+ minimum; (b) $t > 0$; the particle returns to the η_+ minimum and then attempts to hop over the barrier; (c) the particle crosses the barrier and then back to the η_- minimum.

4. Discussion and experimental relevance

4.1. Discussion

The dynamic hysteresis can be understood through a dynamic potential-well model. The state stability for a system is determined by the free energy potential. For a single-loop hysteresis, the free energy has two wells, but three wells exist for the double-loop hysteresis. It can be predicted that the hysteresis may exhibit $N - 1$ close windows if the free energy as a function of order parameter has N potential wells.

Rao *et al* [4] presented a mechanical analogy based on a double-well potential to illustrate the dynamical processes of the spin system in response to a time-varying field. Three characteristic scales of relaxation time were brought out to investigate the relationship of magnetization reversal and external field, as shown in figure 8. The symmetry of the free energy is broken by the applied external field, and the potential wells become inequivalent. For the $(\eta^2)^3$ model, there are two global minima below T_0 , and the system has a similar behaviour as the $(\eta^2)^2$ model. For $T_0 < T < T_c$, the three wells located respectively at η_0 and η_{\pm} are not equivalent to each other and the loop is still a single one. For $T_c < T < T^+$, the triple-well pattern can be treated as two asymmetric double wells, so that the double-loop hysteresis can be regarded as a combination of two single loops.

For a typical double loop, a mechanical analogy for the dynamic hysteresis is shown in figure 9. If an initial stable state at time $t = -T/4 < 0$ is assumed, where T is the period

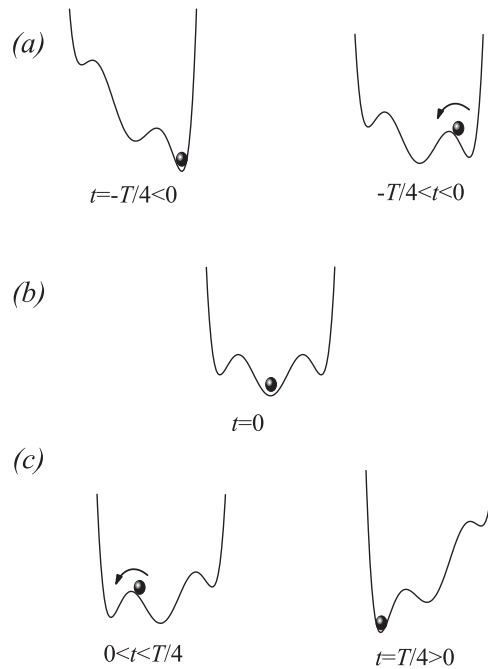


Figure 9. Dynamic triple wells of free-energy potential: (a) initial state, particle is in the η_+ well and then amplitude decays, the particle attempts to hop the barrier to the state η_0 ; (b) $t = 0$, $E = 0$, the particle falls into the η_0 well; (c) the applied field reverses and the well at η_- becomes deeper and then the particle crosses the barrier between η_0 and η_- and falls into the η_- well.

of the external field, $E = E_0 \sin(2\pi f \cdot t) = -E_0$ is at the amplitude value and along the $+\eta$ direction. For $-T/4 < t < 0$, the absolute value of E decreases from E_0 , the difference between $\pm\eta$ becomes smaller and the well at η_0 becomes deeper. At $t = 0$ and $E = 0$, if the system has long enough to relax, the well at η_0 is preferred. The time that the system stays in the disordered state is determined by f . Half of the loop window between $+\eta$ and η_0 is formed. Subsequently, the minimum at $-\eta$ becomes the global minimum. At $t = T/4$ and E along $-\eta$, the well at $-\eta$ becomes the deepest, which leads to formation of the other loop covering η_0 and $-\eta$. When one period is cycled, the same two windows are formed, constituting a double loop.

From the kinetic point of view, the dynamic hysteresis is related to a competition of two timescales: one is the period of the oscillating field and the other is the system relaxation time. Both of them determine the time during which the system stays in the stable state. Given an E_0 , the energy gap between the neighbouring wells remains unchanged. If the oscillating field sweeps too quickly and the system has not enough time to respond to it, a transfer between two neighbouring wells becomes kinetically difficult, leading to a single-loop hysteresis. If the period of the field is equivalent to or longer than the relaxation time, the transfer among the wells is always possible. However, which one of the three wells will be chosen depends on f . If f is very small, the system is quasi-static and has enough time to relax to the lowest-energy well. Otherwise, the limited time does not allow the system to transfer towards the lowest well through the meta-stable states. This is the reason why we see the very different loop shapes for different frequencies. On the other hand, an expansion of the free energy to a higher order than sixth will bring more potential wells and multi-loop hysteresis.

The physics underlying the very different scaling behaviours between $(\eta^2)^2$ and $(\eta^2)^3$ models can be explained using the above picture in a qualitative sense. For the $(\eta^2)^3$ model, there is a coexistence of two phases around T_c , which can be easily seen from the potential well of free energy. The existence of the disordered phase makes the area of the loop, say, the energy loss of the hysteresis in the triple-well potential system, have a different scaling law. With increasing T , the disordered phase plays a more important role, and there is a transition between ordered and disordered phases under the time-varying field. Because the disordered phase exhibits a very thin loop, the loop area will grow at a fast rate with increasing f , resulting in larger scaling exponents at higher temperature. However, as a comparison, a single loop with double wells only has a transition among ordered phases, so the exponent is smaller at lower temperature.

4.2. Experimental relevance

The dynamic hysteresis of ferroelectrics and the domain reversal problem have been given more attention from the experimental point of view. Liu *et al* [24, 25] studied the scaling behaviour of hysteresis dispersion through both model simulation and experiment for $\text{Pb}(\text{Zr}_x\text{Ti}_{1-x})\text{O}_3$ (PZT) at room temperature (far below T_c). The results fit $A \propto E^{0.66} f^{0.33}$ and represent the behaviour of a single loop far below T_c for a first-order phase transition system.

The experiment on double hysteresis for BaTiO_3 was first reported in 1953 [26]. A typical shape evolution of static hysteresis with respect to increasing temperature above T_c was investigated. Systematic comments on the double hysteresis loop in ferroelastic LiCsSO_4 were made on static aspects by Tuszynski *et al* [21]. It is interesting to note the similar values of the scaling exponents between our results near T_c and the antiferroelectric (AFE) double hysteresis loop reported in [27], where power laws $A_H \propto (E_0 - E_c)^{0.5} f^{0.4}$ for AFE double loops and $A_m \propto (E_0 - E_c)^{2.1} f^{0.28}$ for minor loops are given. In section 3, we have presented the scaling exponents for E_0 as 0.5–0.67 at high E_0 and 2.0 at low E_0 . The reason for the similarity, we argue, lies in the fact that AFE also has a triple-well potential, which is very like the potential for $T_c < T < T^+$ in our work. That is, at $\eta_0 = 0$ the system has a minimum and at η_{\pm} it has two higher minima. For FE $\eta_0 = 0$ corresponds to a disordered phase, but for AFE this means an antiferroelectric phase. Although they have quite different physics, the similar free energy potential determines that their hysteresis loss obeys a similar law.

5. Concluding remarks

The dynamic hysteresis in ferroelectric first-order phase transitions near the phase transition point T_c has been studied by an extensive investigation of the hysteresis pattern evolution and scaling behaviours of the $(\eta^2)^3$ model system over wide ranges of both frequency and amplitude of the oscillating external field. In particular, the scaling behaviours of the double-loop hysteresis around T_c have been studied in detail. It has been demonstrated that there is no reliable power-law scaling for the hysteresis area as a function of frequency in the low-frequency regime, while the hysteresis over the high-frequency regime shows a power-law scaling with a frequency exponent $\beta = -1.0$, independent of temperature. For the scaling of the hysteresis as a function of field amplitude, the power law has been confirmed and the amplitude exponent $\alpha = 2.0$ is found for minor loops at small field, although for the saturated loop this exponent takes different values in different temperature regimes. The scaling for the double-loop hysteresis belongs to a generality class different from the single-loop hysteresis, while the dynamics of hysteresis around the phase transition point T_c also differs from that at a temperature far below T_c . The temperature-induced and field-induced phase transitions and two-phase coexistence around T_c cause this distinct difference and complexity. The present

study is valuable for us to understand the non-equilibrium dynamic phenomena near the phase transition point.

Acknowledgments

The authors would like to acknowledge financial support from the National Natural Science Foundation of China through the innovative group project and projects (5017202, 50332020) and the National Key Projects for Basic Research of China (2002CB613303) as well as LSSMS of Nanjing University.

References

- [1] Scott J F 2000 *Ferroelectric Memories* (Berlin: Springer)
- [2] Chakrabarti B K and Acharyya M 1999 *Rev. Mod. Phys.* **71** 847
- [3] Steinmetz C P 1892 *Proc. Am. Inst. Electr. Eng.* **9** 3
- [4] Rao M, Krishnamurthy H R and Pandit R 1990 *Phys. Rev. B* **42** 856
- [5] Rao M and Pandit R 1991 *Phys. Rev. B* **43** 3373
- [6] Jung P, Gray G, Roy R and Mandel P 1990 *Phys. Rev. Lett.* **65** 1873
- [7] Luse C N and Zangwill A 1994 *Phys. Rev. E* **50** 224
- [8] Hohl A, Linden H J C, Roy R, Goldsztein G, Broner F and Strogatz S H 1995 *Phys. Rev. Lett.* **74** 2220
- [9] Acharyya M and Chakrabarti B K 1995 *Phys. Rev. B* **52** 6550
- [10] Fan Z, Zhang J X and Liu X 1995 *Phys. Rev. E* **52** 1399
- [11] Zheng G P and Zhang J X 1998 *J. Phys.: Condens. Matter* **10** 1863
- [12] Dhar D and Thomas P B 1992 *J. Phys. A: Math. Gen.* **25** 4967
- [13] Thomas P B and Dhar D 1993 *J. Phys. A: Math. Gen.* **26** 3973
- [14] Sides S W, Rikvold P A and Novotny M A 1998 *Phys. Rev. E* **57** 6512
Sides S W, Rikvold P A and Novotny M A 1999 *Phys. Rev. E* **59** 2710
- [15] Sides S W, Rikvold P A and Novotny M A 1998 *Phys. Rev. Lett.* **81** 834
- [16] Zhong F and Zhang J X 1995 *Phys. Rev. Lett.* **75** 2027
- [17] Acharyya M and Chakrabarti B K 1993 *Physica A* **192** 471
Acharyya M and Chakrabarti B K 1994 *Physica A* **202** 467
- [18] Bruno P, Bayreuther G, Beauvillain P, Chappert C, Luget G, Renard D, Renard J P and Seiden J 1990 *J. Appl. Phys.* **68** 5759
- [19] Jiang Q, Yang H N and Wang G C 1996 *J. Appl. Phys.* **79** 5122
- [20] Suen J S and Erskine J L 1997 *Phys. Rev. Lett.* **78** 3567
- [21] Tuszynski J A, Mroz B, Kiefte H and Clouter J H 1988 *Ferroelectrics* **77** 111
- [22] Devonshire A F 1949 *Phil. Mag.* **40** 1040
- [23] Mazenko G F and Zannetti M 1985 *Phys. Rev. B* **32** 4565
- [24] Liu J-M, Wang W M, Liu Z G, Chan H L W and Choy C L 2002 *Appl. Phys. A* **75** 507
- [25] Liu J-M, Chan H L W, Choy C L and Ong C K 2001 *Phys. Rev. B* **65** 014416
- [26] Merz W J 1953 *Phys. Rev.* **91** 513
- [27] Kim Y-H and Kim J-J 1997 *Phys. Rev. B* **55** R11933